# Coherent Phononic Balistique Transport and Dynamical Properties of Slab 2D System Waveguides with Structural Defect

Sayhi Mostefa<sup>1</sup>, Bouchareb Sansabilla<sup>1</sup>, Boucherrab Malika<sup>2</sup>, Tigrine Rachid<sup>1,2</sup>, Hachemi. Nadir<sup>1</sup>

<sup>1</sup>Laboratory of energy, environment and information systems, Ahmed Draya Adrar University Algeria 
<sup>2</sup>Laboratory of Quantum Physics and Chemistry, University Mouloud Mammeri of Tizi-

Laboratory of Quantum Physics and Chemistry, University Mouloud Mammeri of Tizi Ouzou, Algeria.

 ${\it Email: sansabilla 123@gmail.com}$ 

We use the a theoretical approach based on the matching method, Landauer-Büttiker and Green formalism to investigate the local phonon density of states (DOS) and the coherent conductance of phonon near the atomic step edge. The model system, containing the atomic step defect, is composed of intersection on three parallel semi-infinite monatomic layers and two parallel semi-infinite monatomic layers. We analysed our model for different cases of elastic hardening and softening. The purpose is to investigate how the local dynamics can respond to changes in the microscopic environment on the perturbed domain. The analysis of the total phonon conductance spectra and the densities of vibration states identify characteristic features and demonstrate the possible use, of atomic step defect, as filters of phonon.

**Keywords:** Localized phonons, step edge defect, transmission and reflection coefficients, density of states, thermal conductivity, thermodynamic properties.

### 1. Introduction

Scattering of elastic waves due to structural defects and nanostructures accumulated in low-dimensional systems is a fundamental problem of interest in solid-state physics. Most of the recent studies in this field [1-3] show the localization mode around the defect region of the perturbation system, resulting in several effects, such as wave reflection, resonance scattering, and localization phenomena [5]. In all cases, the defect leads to an energy trap

and is confined in the vicinity of the regional defect, which occurs in the form of spatially localized phonons. Different experimental techniques have been used to measure the elastic and mechanical properties of low-dimensional systems, in particular surface brillouin light scattering [6], and surface acoustic wave spectroscopy [7].

To address the problems of vibration spectrum and phonon transmission, there are several theoretical and numerical methods in the literature. The matching method is used here[8]. In addition, both the local oscillation mode and the propagation mode scattering can be analyzed within the same mathematical framework. The coherent scattering cross section for phonon transmission is determined as a function of the incident frequency.

The harmonic approximation framework and vibrational waves scattered by atomic step edge inhomogeneity in the nearest and nearest neighbors are studied. The system model is considered to be on a solid surface without interaction with the substrate and consists of atomic step edge intersections between three semi-infinite atomic layers and two semi-infinite atomic layers. In the first step of this work, a complete lattice is investigated (left and right of the perturbation area). In the second stage, defects in the atomic structure are introduced, scattering waves are determined.

The local phonon density of states (DOS) and conductance are obtained and analyzed.

The conductance spectra showed a resonant behavior. In particular, it is shown that this system leads to Fano resonance in the vibrational spectrum. These resonances are due to the coherent coupling between the localized mode near the defect region and the propagated wave of the complete waveguide.

In the next section we present a structural model and we will look at the sec.2 describes the mode of a quasi-one-dimensional waveguide. 3 in seconds. The theoretical form scattering in the perturbation region is given. Sec.4.1 and sec.In 4.2, we present a theoretical model of localized phonon methods and steps, and density of states at the edge, respectively. In Sec5.1 and sec 5.2. Formal thermal conductivity and thermodynamic properties are shown, respectively. Sec6 gives some numerical results and general conclusions.

# 2. THEORETICAL SYSTEM MODEL AND BULK DYNAMICS

The elastic interactions between nearest and next nearest neighbours in the domains to the left and the right of the perturbed zone are represented respectively by the constants k1 and k2, where the shaded area in Fig.1a, constitutes the effective atomic defect domain. The elastic constants in this inhomogeneous boundary may differ from bulk values, and are hence labelled k1d and k2d. It is convenient next to define the following ratios: r = k2/k1, r1d = k1d/k1, r2d = k2d/k1.

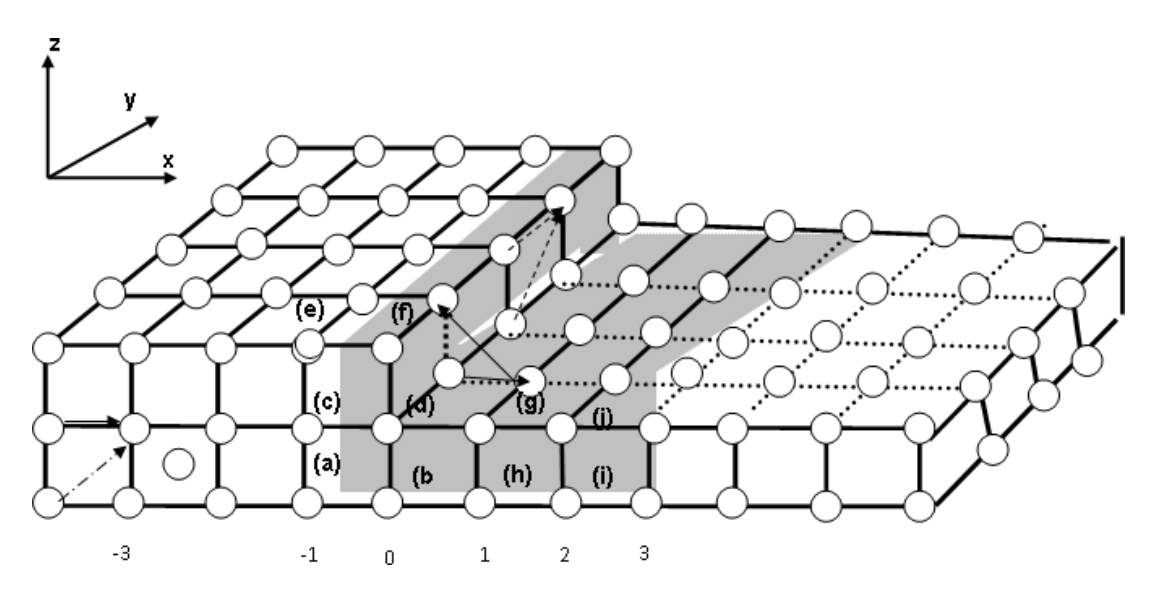


Fig.1a: A schematic representation of a model for an extended atomic step egde in a crystalline solid surface

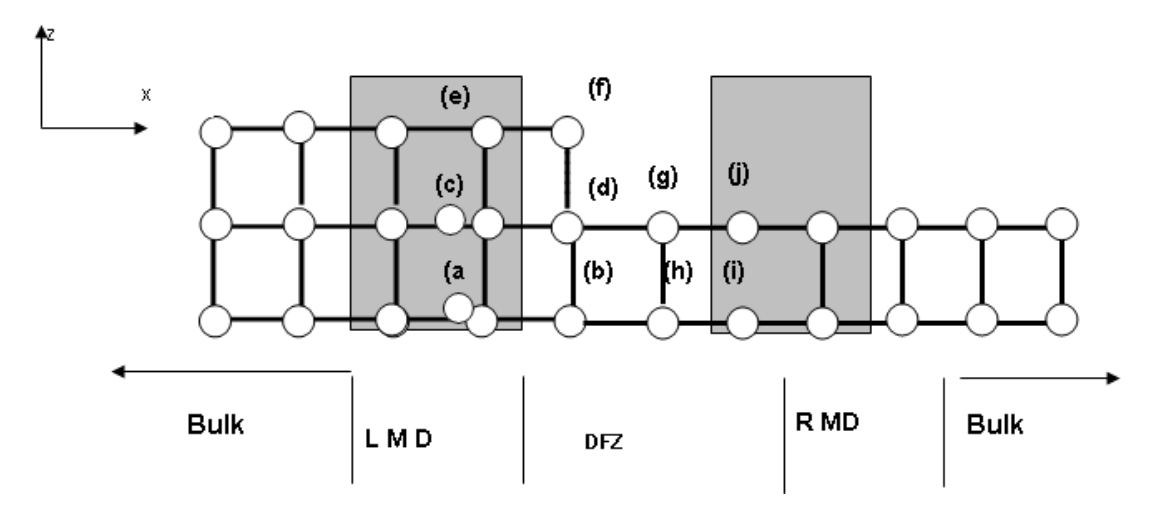


Fig. 1b: The projection of the schematic representation of a model on the plane xoz

The dynamics of the system in the harmonic approximation, [9], are described by the equation of motion of atomic sites l, given by

$$\omega^2 m(l) U_{\alpha}(l) = -\sum_{l' \neq l} \sum_{\beta} k(l,l') r_{\alpha}.r_{\beta}/d^2 \left[ u_{\beta}(l) - u_{\beta}(l') \right] \quad (1)$$

The indices  $\alpha$  and  $\beta$  denote Cartesian co-ordinates, m(l) is the atomic mass for site l, and  $u_{\alpha}(l)$  is the corresponding displacement vector vibration, of the l atom. The radius vector r between the atomic sites at l and l', has Cartesian components  $r_{\alpha}$ , and d = |r|. The force constant between the two sites is k(l,l').

For sites 1 and 1' distant from the inhomogeneous boundary to the left and right of the *Nanotechnology Perceptions* Vol. 20 No.6 (2024)

interval  $n \in [-2,2]$  of Fig. 1, the equations of motion may be cast, in the matrix form

$$[\Omega^{2}I - D(\eta, k_{1}, k_{2})]|U>=0$$
(2)

D is a (6×6) matrix, and  $|U\rangle$  is the corresponding displacement vector for a column of the perfect waveguide, and  $\eta$  is the phase factor.

To illustrate the model, the propagating modes for the perfect waveguides are presented in Fig.2 for a choice of r=0.75, as a function of the normalized wave vector  $\phi_x=k_x a$ , where  $\phi_x$  runs in the interval  $[-\pi,\pi]$  over the first Brillouin zone and a is the interatomic distance between adjacent lattice sites.

There are two acoustical modes  $\Omega_1$  and  $\Omega_2$  characterized by the limiting behaviour of their phonon branches, tending to zero frequency when the wavevector tends to zero, and four optical modes with branches that differ from zero in the long-wavelength limit.

### 3. THE SCATTERING PROBLEM AT STEP EDGE

In order to render the problem tractable we need to decouple the dynamics of a representative and irreducible set of sites at the inhomogeneous boundary of the perturbed domain from the rest of the system. The represented sites of the step edge set are comprised as in Fig.1a, from the sites labelled (a), (b), (c), (d), (e), (f), (g), (h), (i). and (j).

The matching method [10–12] provides a framework for the calculation of the localized modes as well as of the spectral densities. We are able to calculate the localized modes. In this paper, however, the results for the localized mode are not presented. Our main interest here is to calculate the spectral densities and the phononic conductance.

For an incoming propagating wave corresponding to the eigenmode i at a frequency  $\Omega$  and incident from the left to right, the resulting scattered waves at  $\Omega$ , are composed of a reflected and a transmitted part. The Cartesian components  $\alpha$  of the displacement field U(n,n') for an outside atom bordering the defect domain [-2, 2], may be expressed using the matching approach. For a site inside the waveguide to the left of the defect, the displacement field  $U_{\alpha}(n,n')$  can be expressed as the sum of the incident wave and a superposition of the eigenmodes of the perfect wave guide reflected at the same frequency

$$U_{\alpha}(\mathbf{n},\mathbf{n}') = \mathbf{u}_{i}\eta_{i}^{n} + \Sigma_{i}\eta_{i}^{-n}\mathbf{R}_{ii}\mathbf{u}_{i} \text{ with } \mathbf{n} \leq 2$$
(3)

Where the vectors  $u_i$  denote the eigenvectors of the dynamic matrix for the perfect waveguide at the frequency  $\Omega$ .  $R_{ij}$  are the reflection coefficients that describe the scattering of a given incident wave i into the eigenmodes j=1,2,3,4,5,6. For a site inside the wave guide to the right of the defect, the displacement field  $U_{\alpha}^{+}(n,n')$  can be expressed by an appropriate superposition of the eigenmodes of the perfect wave guide transmitted at the same frequency

$$U_{\alpha}^{+}(\mathbf{n},\mathbf{n}') = \Sigma_{\mathbf{j}} \eta_{\mathbf{j}} {}^{\mathbf{n}} T_{\mathbf{i}\mathbf{j}} u_{\mathbf{j}} \qquad \text{with} \quad \mathbf{n} \ge 2$$
 (4)

 $T_{ij}$  are the transmission coefficients for incident wave i into the eigenmodes j = 1, 2, 3, 4, 5, 6.

Consider a Hilbert space for the scattering and denote by [|R>, |T>] the basis vector

for the reflection and transmission coefficients in this space, and by  $|U\rangle$  that for the displacements of a set of irreducible sites in the defect domain. The equations of motion for the defect, coupled to the rest of the systems, may be written in terms of vector  $[|U\rangle, |R\rangle, |T\rangle$ ]. Using the transformations connecting the displacement fields in Eqs.(3)-(4), we obtain a square linear inhomogeneous system of the equations of the form

$$[\Omega^{2}I - D_{m}(\eta, r, r_{1d}, r_{2d})] [|U\rangle, |R\rangle, |T\rangle] = -|IH\rangle$$
(5)

Where the vector -|IH>, mapped appropriately onto the basis vectors, regroups the inhomogeneous terms describing the incoming wave.

The solution of Eq.(5) yields the displacements  $|U\rangle$  of the irreducible set of atomic sites for the defect domain [-2, 2], as well as the reflection and transmission coefficients  $R_{ij}$  and  $T_{ij}$  on the perfect wave-guides.

The scattering behaviour is usually described in terms of the scattering matrix, which elements are given by the relative reflection and transmission probabilities  $r_{ij}$  and  $t_{ij}$  at the scattering frequency  $\Omega$ . These are given by

$$r_{ij} = (V_{gi} / V_{gi}) | R_{ij} |^2$$
 and  $t_{ij} = (V_{gj} / V_{gi}) | T_{ij} |^2$  (6)

Where in order to obtain unitarity of the scattering matrix, the scattered waves have to be normalised with respect to their group velocity. Vgs is the group velocity of the eigenmodes, put equal to zero for evanescent modes.

We can further define total reflection and transmission probabilities for a given eigenmode at scattering frequency  $\Omega$  by summing over all the contributions

$$r_i(\Omega) = \sum_i r_{ii}(\Omega)$$
 and  $t_i(\Omega) = \sum_i t_{ii}(\Omega)$  (7)

Furthermore, in order to describe the over all transmission of mesoscopic multichannel systems at a given frequency  $\Omega$ , it is useful to define the conductance of the system (or the domain defect transmittance)  $t(\Omega)$ , by summing over all input and output channels

$$t(\Omega) = \sum_{i} \sum_{j} tij(\Omega)$$
 (8)

The sum is carried out over all propagating modes at frequency  $\Omega$ . The transmission probabilities  $t_i(\Omega)$  per eigenmode i, and the conductance of the system  $t(\Omega)$ , are important to calculate because each corresponds indeed to an experimentally measurable observable.

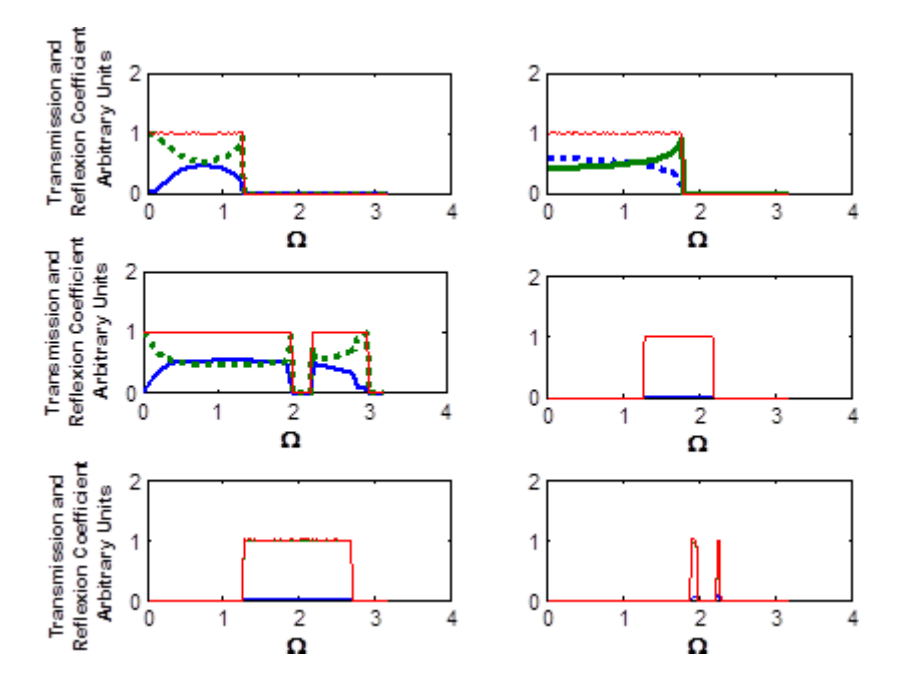


Fig.4 . Curve of the transmission and reflection coefficients as the dimension less frequencies  $\Omega$  and the parameter of the system at neighborhood of the defect of the model

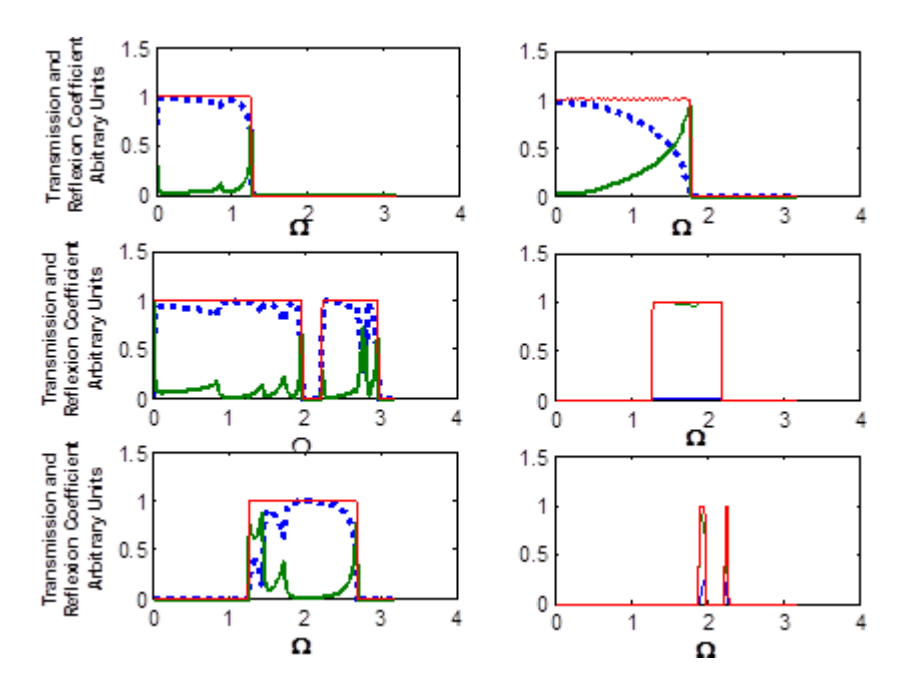
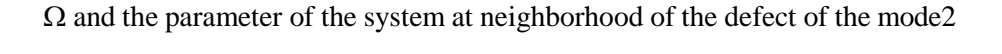


Fig.5: Curve of the transmission and reflection coefficients as the dimension less frequencies



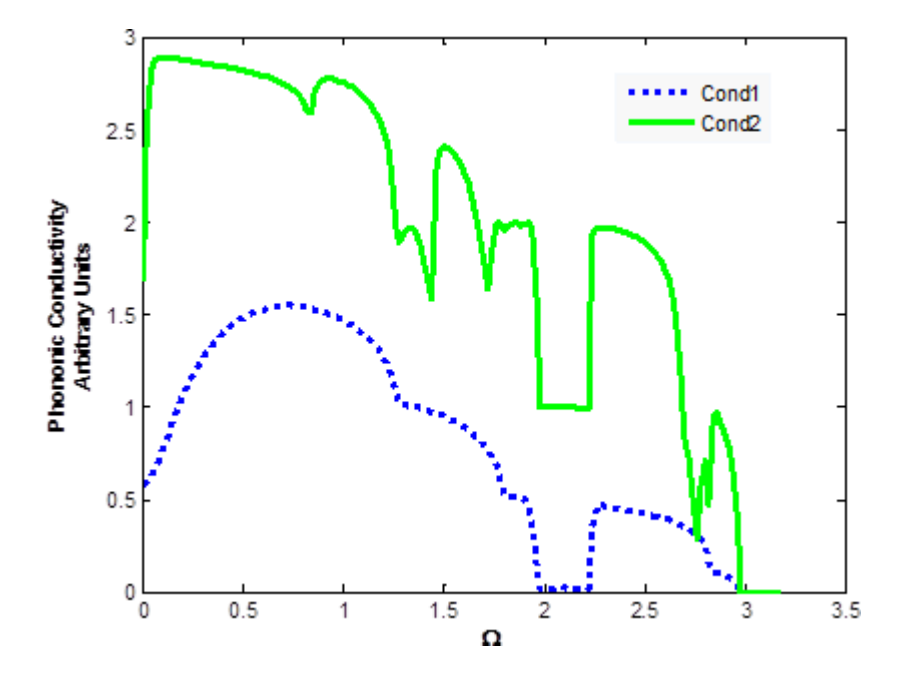


Fig.6 .Curve of the phononic conductance as function the dimension less frequencies  $\Omega$  and the parameter of the system at neighborhood of the defect of the model

# 4. 1.LOCALIZED PHONONS AT THE STEP EDGE

Consider the Cartesian x, y, and z-axes, referring to Fig.1a, as respectively parallel to the directions [100] normal to the step edge,  $[\bar{1}\ 00]$ 

The the edge is next considered. This breaks the translation symmetry along the x axis normal to its plane. To describe the step edge dynamic effects, there is need to consider both the propagating and the evanescent eigenmodes along this axis. The eigenmodes are then described in a general manner by the phase doublets  $\{\eta_x \ \eta_x^{-1}\}$  normal to the defect. The propagating phonons satisfy the condition  $|\eta_x|=1$  whereas the evanescent eigenmodes are determined from the condition  $|\eta_x|<1$ . The nontrivial doublet solutions  $\{\eta_x, \ \eta_x^{-1}\}$  are calculated, as a function of the frequency  $\Omega$ , and of the force constants of the system, from the solutions of the secular equation for the resultant matrix

$$[\Omega^2 I - D(e^{i\phi y}, \eta_x, r)], [15].$$

Since the dynamics of the step edge generate an infinite system of coupled equations, the dynamics of an irreducible set of sites at the step edge need to be decoupled appropriately from the rest of the system, in order to render the problem tractable, [13]. In the matching domains at the left and the right of the defect, the vibration displacements  $u_{\alpha}$  for an atom may be expressed in a constructed Hilbert space over the basis vectors  $|R\>\rangle$  of the Nanotechnology Perceptions Vol. 20 No.6 (2024)

evanescence field. Using Eq.4 for the surface vibrations, and the transformations mapping the two vectors  $|R\rangle$  and  $|u\rangle$ , we obtain a system of linear equations

$$[D_m(e^{i\phi y}, \eta_x, \Omega, r)] | u, R > = |0>,$$
 (9)

where  $[D_m(e^{i\phi y}, \eta_z, \Omega, r)]$  is a characteristic square matrix, calculated in the matching formalism. The dimensions of this matrix are characteristic of an irreducible set of sites at the surface boundary, and of the size of the constructed Hilbert

space for the matching domain between the surface and the bulk. The matching formalism provides a framework for the calculation of the localized modes and of the spectral densities at the step edge..

By diagonalizing the matrix  $[D_m(\ e^{i\phi y}\ ,\ \eta_x,\ \Omega,\ r)]$ , we are able to calculate the Rayleigh phonons that propagate in the high symmetry direction oy and which essentially decay exponentially into the bulk. We assume that the force constants are unaltered in the defect. They are calculated here for the step edge along the [010] direction, and are presented in Fig.7. We identify an optic non dispersive Einstein mode, clearly visible in Fig.7 which are situated under the bulk band frequencies.

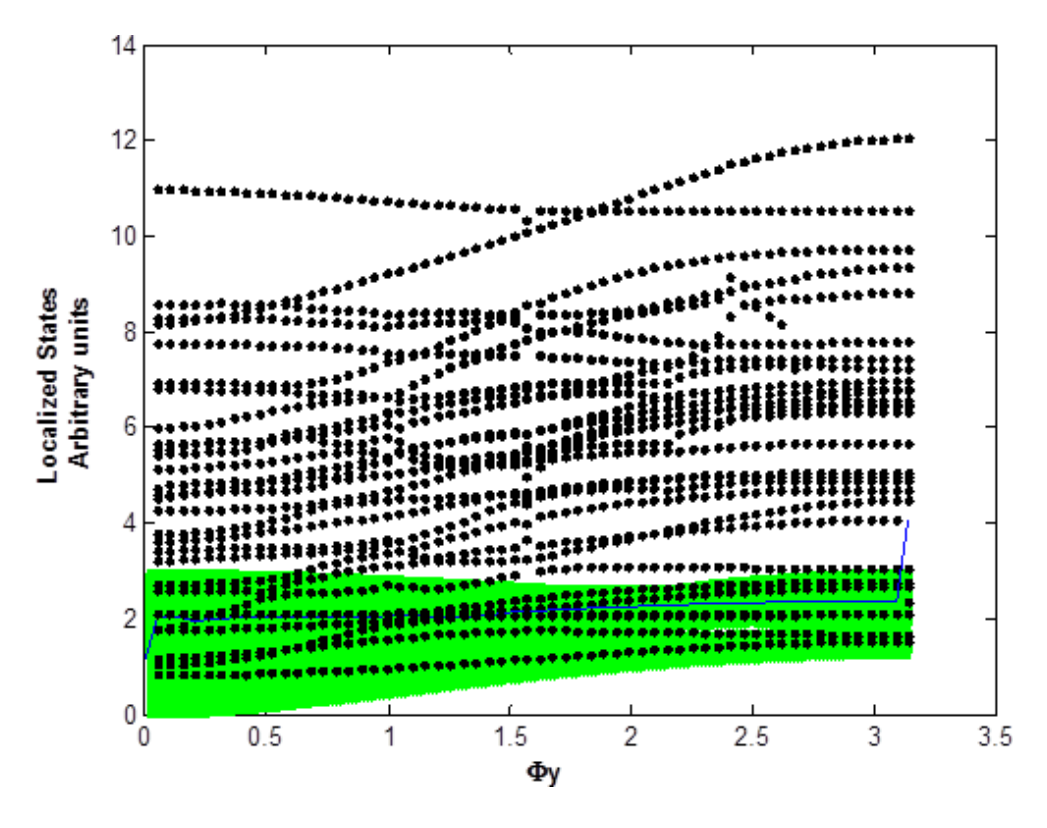


Fig.7: Localized phonons at the step edge as function the dimension less frequencies  $\Omega$  and the parameter of the system at neighborhood of the defect.

# 4.2. STATE DENSITY AT THE ATOMIC DEFECT

The most direct manner to calculate the spectral densities is via the Green's functions, which may be expressed formally [13], using equation (5), as

$$G(\Omega^2 + i\varepsilon) = \left[ (\Omega^2 + i\varepsilon)I - D_m(\eta, r, r_{1d}, r_{2d}) \right]^{-1}$$
(10)

The vibration density of states (DOS) per atomic site l, is obtained next as a sum over the trace of the spectral density matrix.

$$N_{l}(\Omega) = -2\Omega/\pi \sum_{\alpha} \lim(\lim[G^{l}_{\alpha\alpha} (\Omega^{2} + i\varepsilon)])$$
(11)

The vibration spectra are calculated and presented for the different sites of the perturbed domain in the following section.

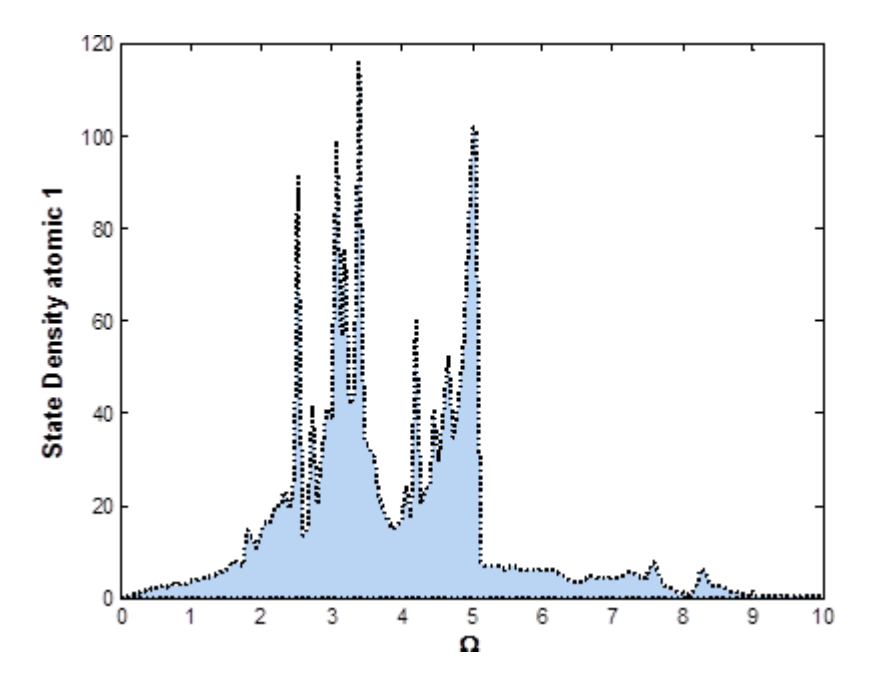


Fig.8: State density of Localized phonons at site  $1 \equiv (b)$  of the step edge as function the dimension less frequencies  $\Omega$  And the parameter of the system at neighborhood of the defect

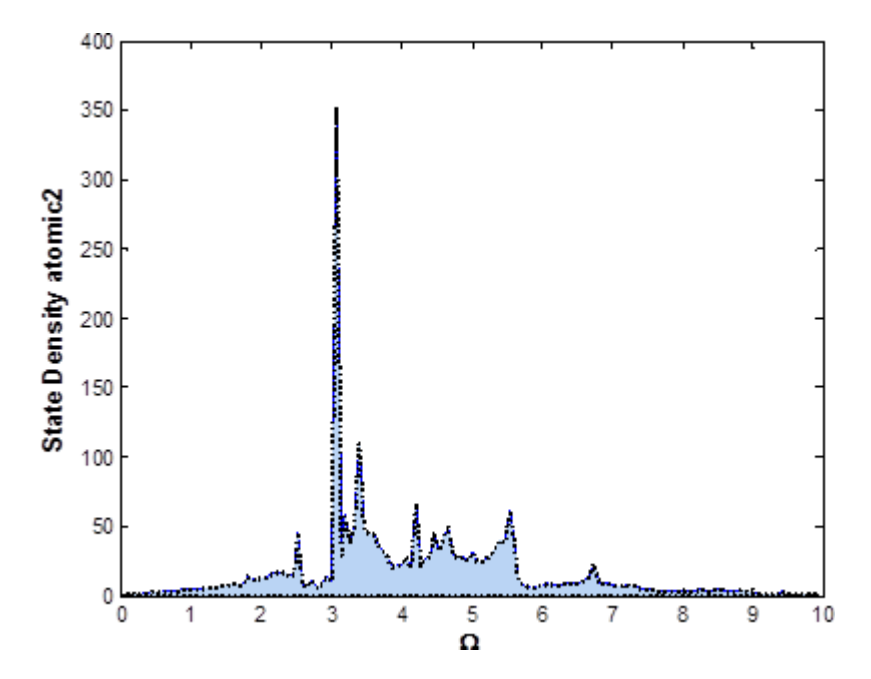


Fig.9: State density of Localized phonons at site  $2 \equiv (d)$  of the step edge as function the dimension less frequencies  $\Omega$  And the parameter of the system at neighborhood of the defect

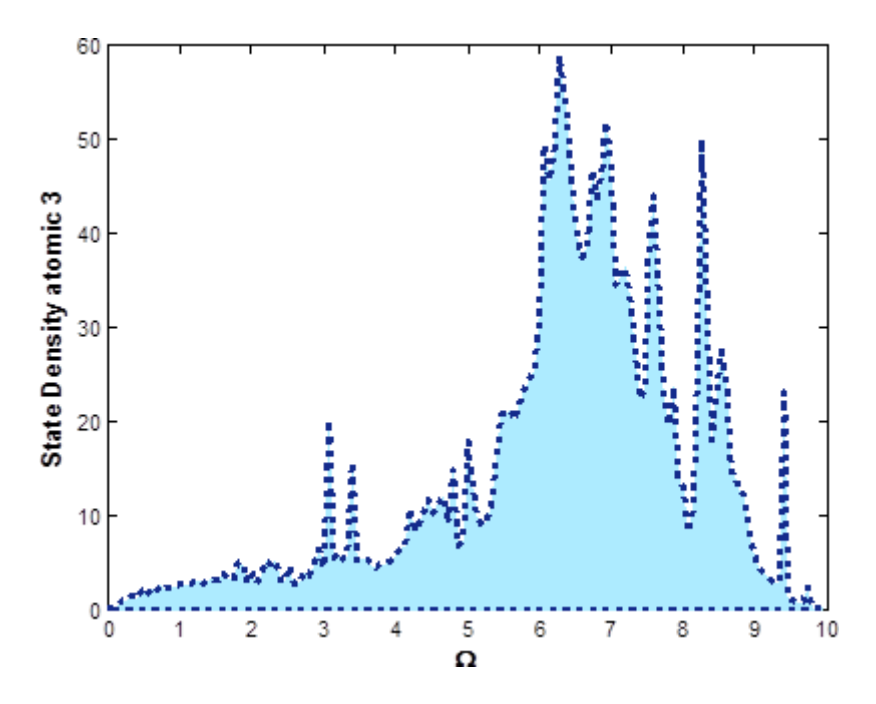


Fig.10: State density of Localized phonons at site 3 = (f) of the step edge as function the

dimension less frequencies  $\Omega$  And the parameter of the system at neighborhood of the defect

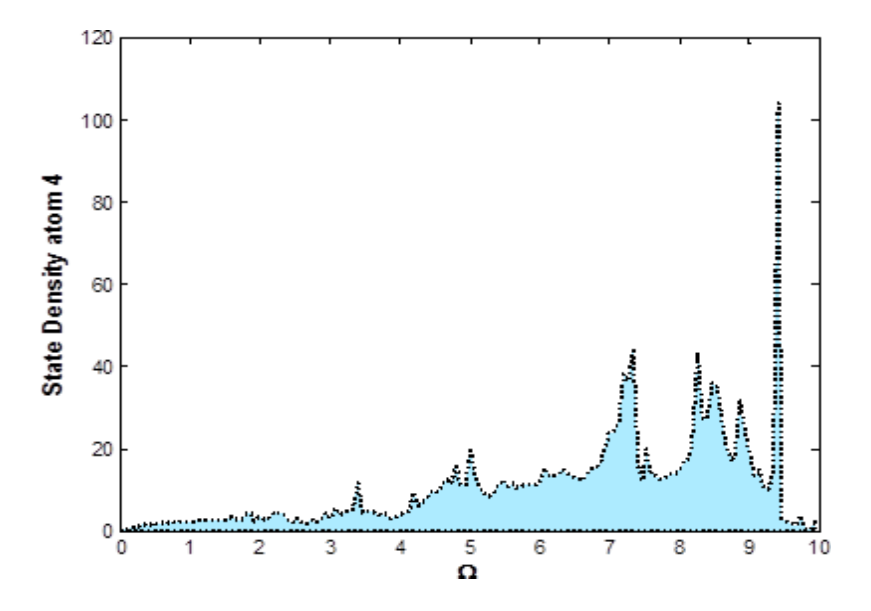


Fig.11: State density of localized phonons at the  $4 \equiv (g)$  site of the step edge as function of dimension less frequencies  $\Omega$  and the parameters of the system at neighbourhood of the defect

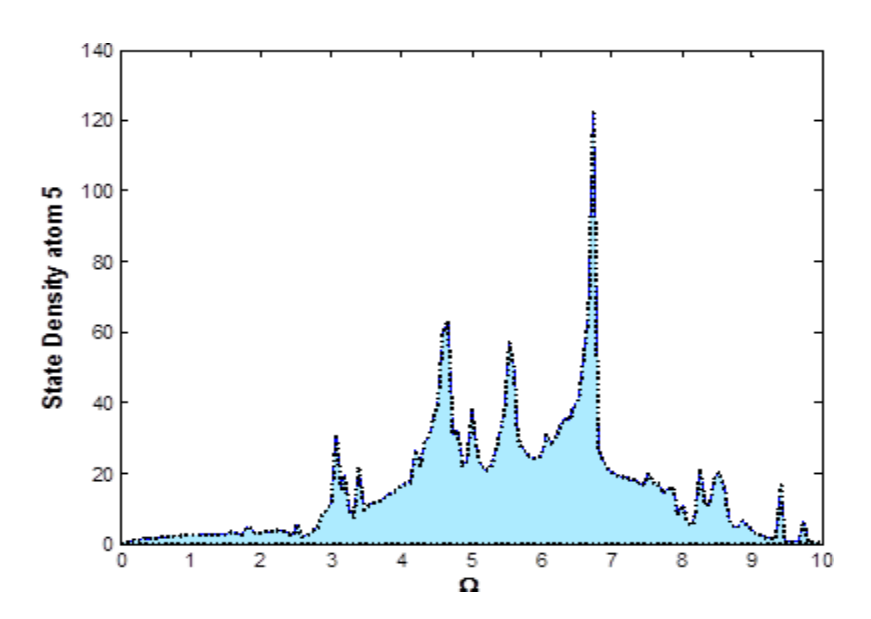


Fig.12: State density of Localized phonons at site  $5 \equiv$  (h) of the step edge as function the dimension less frequencies  $\Omega$  And the parameter of the system at neighborhood of the defect $\equiv$ (b)

### 5.1. THERMAL TRANSPORT VIA THE ATOMIC STEP EDG

In this part, we will develop the numerical results of the study of the thermal conductivity of phonons through the atomic junctions connecting three and two semi-infinite layers waveguides. The calculation process was carried out by analogy with the calculations developed by R. Landauer for the study of electronic transport. Our work will be oriented directly towards the study of the reduced thermal conductivity  $K_r = 2\pi K/k_B\omega_0$  as a function of the reduced temperature  $T_r = k_B T/\hbar\omega_0$  using the formula (13) given in the third chapter. The study will include the effect of the length of the atomic defect, the angle of incidence of the exciting wave  $\varphi_y$ . We will obtain a final expression for the thermal conductivity of the form

$$K = \frac{k_B \omega_0}{2\pi} \cdot \left(\frac{h\omega_0}{k_B T}\right)^2 \sum_{v} \int_{0}^{\infty} \Omega^2 \cdot \frac{e^{h\omega_v \Omega_v / k_B T}}{(e^{h\omega_v \Omega_v / k_B T} - 1)^2} \cdot \sigma(\omega) \cdot d\Omega$$
(12)

We define the reduced temperature by:  $T_r = k_B T / \bar{h}\omega_0$  and the reduced thermal conductivity as follows:  $K_r = 2\pi K / k_B \omega_0$ . The expression (12) becomes

$$K_{r} = \sum_{v} \int_{0}^{\infty} \frac{\Omega_{v}^{2} - e^{\Omega_{v}/T_{r}}}{T_{r}^{2} \left(e^{\Omega_{v}/T_{r}} - 1\right)^{2}} \cdot \sigma_{v}^{(\omega)} \cdot d\Omega_{v}$$
(13)

The Figures represent the variation of the reduced thermal conductivity of the system perturbed by the atomic step edge connecting the two perfect waveguides, as a function of reduced temperature for a variety of system parameters.

The reduced thermal conductivity which is defined as being the integral over the entire range of propagation of the vibration modes, to within a factor, of the product of the square of the Bose distribution with the phononic conductance. It is proportional to the reduced temperature, it starts with zero for low temperatures then increases until reaching a maximum value which differs depending on the system parameters.

In Figure, we have shown the influence of the atomic defect on the reduced thermal conductance of the system, in the case of a ratio of elastic constants We notice that the maximum thermal conductivity is better for the length and reaches approximately , then gradually decreases in decreasing the length of the atomic wire until reaching approximately in the case of the length . Therefore, we can say that the reduced thermal conductivity is proportional to the length of the atomic step edge.

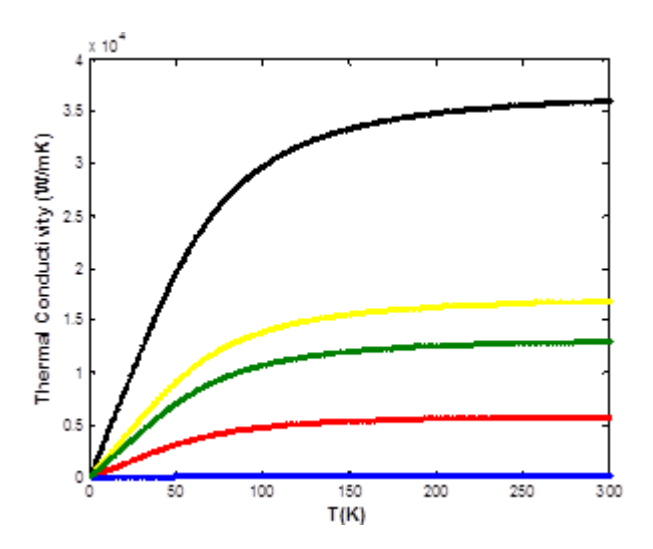


Fig.13: Thermal conductivity of the step edge as function the temperature and the parameter of the system at neighborhood of the defect

# 5.2. THERMODYNAMIC PROPERTIES.

Phonons, rooted in the foundations of quantum mechanics and embodying the principle of wave-particle duality, exert a profound influence on a plethora of solid-state properties. These include critical thermal attributes such as vibrational specific heat [14, 15], vibrational free energy, vibrational internal energy [16-18], and vibrational entropy [19-21]. Consequently, the theory of lattice vibrations [36-44 becomes indispensable for the inclusion of phonon contributions in the computation of thermodynamic properties.

Within the realm of statistical physics, the partition function Z serves as a cornerstone concept that facilitates the deconvolution of the composite system into its harmonic oscillators. This leads to a scenario where the partition function manifests as the product of the individual partition functions corresponding to each vibrational mode [22, 23]. The expression for this pivotal function is articulated as follows:

$$Z = \sum_{n_{\mathcal{S}(q)}} e^{-\frac{E_{(q,s)}}{K_B T}} \tag{14}$$

The density of states is recognized as an exceptionally utilitarian metric in the realm of physics[45-55], not only for its direct measurability but also for its conceptualization as a continuous function in the context of the thermodynamic limit. This facilitates the calculation of a myriad of thermodynamic properties, contingent upon the computation of the vibrational density of states, thus serving as a vital precursor to further thermodynamic inquiry [24-25].

In the framework of thermodynamics, the total energy of a system, commonly referred to as the internal energy (U or E), particularly within a volume where the particle count is held constant to preserve unchanged energy levels, is intricately linked to and derivable from the partition function Z. The relationship between the internal energy and the partition function is not only fundamental but also quantifiable, allowing for a robust method to compute the *Nanotechnology Perceptions* Vol. 20 No.6 (2024)

internal energy [26]:

$$U = \frac{\partial LogZ}{\partial \beta} \tag{15}$$

Considering the density of vibrational states  $D(\omega)$ , the internal energy U is transformed into the form [27]:

$$U_{vib} = K_B T \int_0^\infty \left(\frac{\hbar w}{K_B T}\right) \cdot \coth\left(\frac{\hbar w}{K_B T}\right) \cdot D(w) dw$$
 (16)

The free energy F of a system can be expressed as:

$$F_{vib} = K_B T \int_0^\infty Ln\left(2.\sinh\left(\frac{\hbar w}{2K_B T}\right).D(w)dw$$
 (17)

The cohesive interrelation that seamlessly ties the free energy and internal energy in a thermodynamic system paves the way to unearth a pivotal thermodynamic quantity: the Vibrational Entropy, denoted as  $S_{vib}$ . Mathematically, vibrational entropy is expounded as:

$$S_{vib} = K_B T \int_0^\infty \left[ \left( \frac{\hbar w}{K_B T} \right) \cdot \coth \left( \frac{\hbar w}{K_B T} \right) - Ln 2 \sinh \left( \frac{\hbar w}{2K_B T} \right) \right] D(w) dw \tag{18}$$

Vibrational entropy[56-61] is distinctively defined as a thermodynamic variable intrinsically associated with a system's state of particulate constituents. Its quintessential role is to quantify the level of disorder or the extent of randomness present within a system. Embracing the postulate that entropy exists as a tangible attribute, particularly in the analysis of a substantial aggregate of particles conceived as a continuum, we proceed to its quantification within the thermodynamic limit. The introduction of the vibrational density of states function ( $\omega$ ) permits the establishment of an expression for vibrational entropy, providing a formulaic representation of this concept [28-31]:

$$S_{vib} = K_B \int_0^\infty \left[ \left( \frac{\hbar w}{K_B T} \right) \cdot \coth \left( \frac{\hbar w}{K_B T} \right) - Ln 2 sinh \left( \frac{\hbar w}{2K_B T} \right) \right] D(w) dw \tag{19}$$

Specific heat, another essential material property, involves two primary forms of energy conduction in a solid; electronic and through atomic vibrations. Focusing on the phonon contribution (atomic vibration) and specifically the specific heat at constant volume due to its fundamental nature for solids, it is definded by [32-35]:

$$C_{vib} = K_B \int_0^\infty \left[ \left( \frac{\hbar w}{K_B T} \right)^2 \cdot \frac{1}{\sinh^2 \left( \frac{\hbar w}{2K_B T} \right)} \right] D(w) dw$$
 (20)

It's crucial to note that the vibrational specific heat encompasses the energy density variation associated with network vibrations as per temperature. The total system energy, encompassing the contributions of all particles within the system, is derived concerning the temperature T.

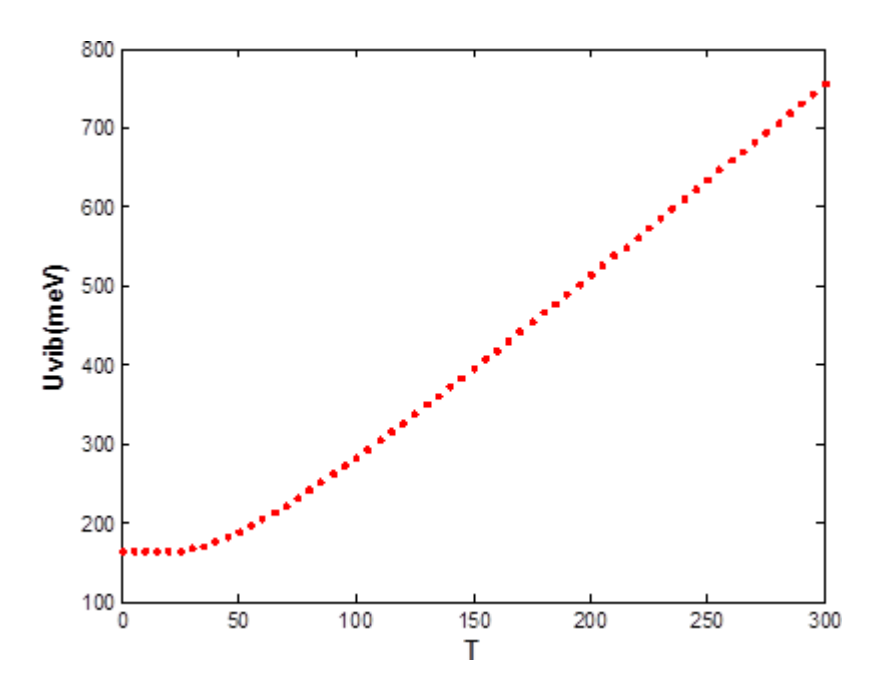


Fig 14: Internal Energy (U) as a Function of Temperature T and the parameters at the defect

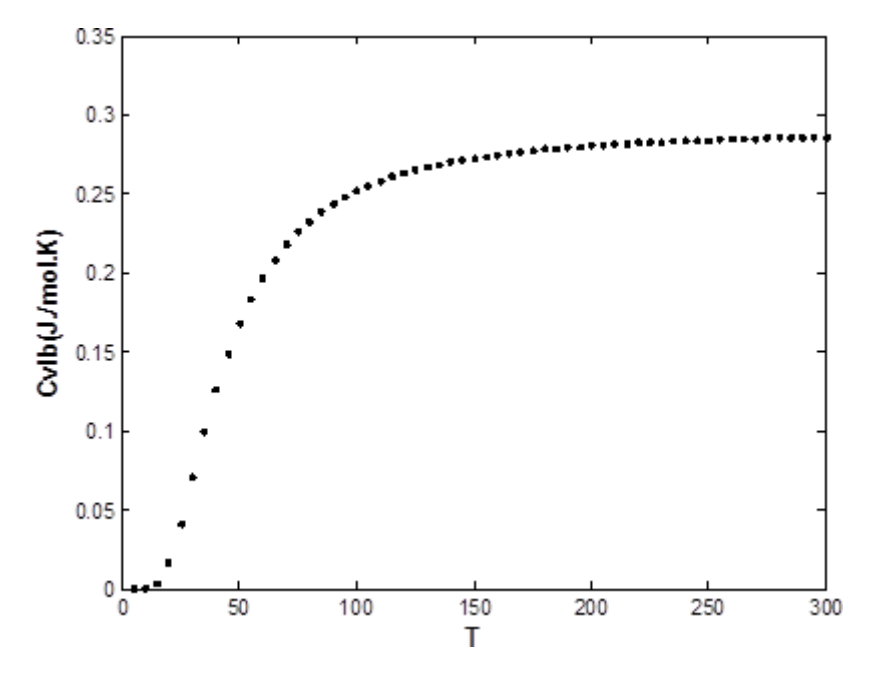


Fig 15: Vibrational Specific Heat as a Function of Temperature T and the parameters at the defect

# 6. NUMERICAL APPLICATIONS AND CONCLUSIONS

The step edge monatomic defect, are presented in Fig.1a. The perturbed domain is taken on gray area. The scattering of the phonons at the domain defect is studied with reference to incident vibrational waves of the perfect wave-guide, which is split into its transmitted and reflected parts.

The results presented in this section are obtained with reference to phonons incident from the left of the domain defect to right in Fig.1a. The numerical analysis is carried out for three different cases determining a choice of the elastic properties of the perturbed domain.

- (i)  $r_{1d}$ =0.9, r=0.75,  $r_{2d}$ =0.65
- (ii)  $r_{1d}=1.0$ ,  $r_{2d}=r=0.75$
- iii)  $r_{1d}=1.1$ , r=0.75,  $r_{2d}=0.85$ .

Which is a reasonable possibility (softening, homogeneous and hardening).

The states density (DOS) for the above sites, are presented in figure 4, for the individual sites, (a), (b) (c), (d),(e),(f), (g) and (h) from top to bottom, and are arranged so that the columns from left to right correspond to the cases (i), (ii) and (iii). There is evidence with reference to the DOS, for a localized collective resonance about  $\Omega \cong 0.5$  for the ensemble of the irreducible sites of the nano domain.

It is observed that the energy line of this mode goes to higher frequencies with increasing hardness of the elastic constants:  $\Omega = 0.45$  for (i),  $\Omega = 0.50$  for (ii),  $\Omega = 0.55$  for (iii).

The changes in  $\Omega$  are of the order of magnitude of the changes considered for the elastic constants of the nanocontact domain, which leads us to the conclusion that this mode would correspond primarily to a collective vibration of the nanocontact domain in the potential step edge.

The corner sites (8, 11) do not present any other features attesting to more of a role of confinement for the nanocontact domain. The analysis of their DOS yields a number of further conclusions.

In contrast, the pair of sites (3, 5) present a specific resonance lines, at  $\Omega = 1.25$ , that do not show up for any of the other sites in the nanocontact domain. We interpret this by assigning these resonance lines to collective localized vibration modes of the pair of sites (3, 5) against the rest of the system where all sites remains stationary.

In conclusion, we have presented a simple model for the study of the vibration spectra of an atomic nanocontact which acts as the joint between two sets of semi-infinite monatomic chains. It enables one to address questions regarding the mechanical properties of nanocontacts. The analysis of the vibration spectra and of the DOS of the set of irreducible sites in the nanocontact domain demonstrates the central role of a core subset of these sites for the dynamics of the nanocontact. It can also serve towards the study of granular chains constructed in an analogous manner on the classical macroscopic scale.

# References

- [1] M. Büttiker, Phys. Rev. Lett. 57, 1761 (1986)
- [2] V. R. Velasco, F. Garcia-Moliner, L. Miglio, L. Colombo, Phys. Rev. B 38,3172 (1988)
- [3] M. Belhadi, A. Khater, J. Hardy and K. Maschke, Eur. Phy. J. Appl. Phys. 35, 185 (2006)
- [4] B. Bourahla, A. Khater, O. Rafil and R. Tigrine, J. Phys.: Condens Matter 18, 8683 (2006)
- [5] I. M. Lifshitz and A.M. Kosevich, Rep. Prog. Phys. 29, 217 (1966)
- [6] R. Danner, R. P. Huebener, C. S. I. Chun, M. Grimsditch, I.K, Schuller, Phys. Rev. B33, 3696 (1986)
- [7] A. Neubrand, P. Hess, J. Apl. Phys., 71, 227 (1992)
- [8] J. Szeftel, A. Khater, J. Phys. C 20, 4725 (1987)
- [9] F. Gagel and K. Maschke, Phys. Rev. B52, 2013(1995).
- [10] J. Szeftel, A. Khater, F. Mila, S. D'addato and N, Auby, J. Phys. C: Solid St. Phys. 21, 2113 (1988)
- [11] Y. Pennec, and A. Khater, Surf. Sci. Lett. 348, 82 (1995)
- [12] A. Fellay, F. Gagel, K. Maschke, A. Virlouvet and A. Khater, Phys. Rev. B 55, 1707 (1997)
- [13] H. Grimech and A. Khater, Surf. Sci. 323, 198 (1995)
- [14] S.V. Eremeev, G.G. Rusina , E.V. Chulkov, Diffusion properties of Cu(0 0 1)-c(2  $\times$  2)–Pd surface alloys, Surf. Scie.601, 3640 -3644(2007).
- [15] J. Sun, J. B. Hannon, G. L. Kellogg, and K. Pohl, Local structural and compositional determination via electron scattering: Heterogeneous Cu(001)-Pd surface alloy, Phys. Rev. B. 76,205414 (2007).
- [16] L. Li, K. Xun, Y-m Zhou, D-s Wang, and S-c Wu, First-principles calculation of the atomic and electronic structure of the surface alloy Cu(001)c(2×2)–Pd,,Phys. Rev. B. 71, 075406 (2005).
- [17]N. P. Blanchard, D. S. Martin, A. M. Davarpanah, S. D. Barrett, and P. Weightman, Pd Deposition onto the Thermally Roughened Cu(110) Surface, Phys. Stat. Sol. (a). 188, N° 4, 1505–1512 (2001).
- [18] R. A. Bennett, S. Poulston, N. J. Price, J. P. Reilly, P. Stone, C. J. Barnes, and M. Bowker, Surf. Scie.433-435, 816 (2002).
- [19] P. W. Murray, S. Thorshaug, I. Stensgaard, F. Besenbacher, E. Lægsgaard, A. V. Ruban, K. W. Jacobsen, G. Kopidakis, and H. L. Skriver, Phys. Rev. B.55, N°03, 075428
- [20] Feuchtwang T E 1967 Phy. Rev.155 731
- [21] Szeftel J and Khater A 1987 J. Phys. C: Solid St. Phys. 20 4725
- [22] Khater A, Rafil O, Labaye Y and Pennec Y 1993 Solid St. Comm.87 53
- [23] Virlouvet A, Grimech H, Khater A, Pennec Y and Maschke K 1996 J. Phys.: Cond. Matter8 7589
- [24] Tigrine R, Khater A, Belhadi M and Rafil O 2005 Surf. Sci.580 1
- [25] Bourahla B, Khater A and Tigrine R 2009 Thin Sol. Films 517 6857
- [26] Maradudin A, Wallis R F and Dobrzynski L 1980 Handbook of Surfaces and Interfaces Vol 3 (New York)
- [27] Grimech H and Khater A 1995 Surf. Sci.323 198
- [28] E. Wimmer 2005 Mat. Sci.-Poland23 325
- [29] Wu E J, Ceder G and van de Walle A 2003 Phys. Rev. B67 134103
- [30] Sklyadneva I Y, Rusina G G and Chulkov E V 2003 Phys. Rev. B68 045413
- [31] Li L, Xun K, Zhou Yu-M, Wang D.-S and Wu S.-C 2005 Phys. Rev. B71 075406
- [32].A.Khater, R.Tigrine, and B.Bourahla, Phys. Status Solidi B 246, No. 7, 1614–1617 (2009)
- [33].A. Kara, S. Durukanoglu and T.S. Rahman, phy. Rev. B. 53, 15489 (1996).
- [34].S. Iikubo, H. Ohtani and M. Hasebe, Material. Transaction. 51, 574 (2010).
- [35].H.L. Yu, G.W. Yang, Y. Xiao, X.H. Yan, Y.L. Mao, Y.R. Yang and Y. Zhang, Chem. Phys. Letts. 417, 272 (2006).
- [36].I. Atanasov and M. Hou, Phys. Stat. Sol. C. 7, 2604 (2010).

- [37].W. Fei, A. Kara and T.S. Rahman, phy. Rev. B. 61, 16105 (2000).
- [38].C. Kittel, Physique de l'État solide, 7e Éd. Dunod, Paris (1998).
- [39].N.W. Ashcroft and N.D. Mermin, Physique des solides, EDP. Sciences, Paris (2002).
- [40].H.T. Diep, Physique de la Matière Condensée, Dunod, Paris(2003).
- [41].C. Ngô, H. Ngô, Physique statistique, 3e Éd. Dunod, Paris (2007).
- [42].S. Vauclair, Eléments de physique statistique, interEditions, Paris (1993).
- [43].T.S. Rahman, J.D. Spangler and A. Al-Rawi, J. Phys. Condens. Matter. 14, 5903 (2002).
- [44].H.Yildirim, A. Kara and T.S. Rahman, J. Phys. Condens. Matter. 21, 084220 (14pp) (2009).
- [45].S. Durukanoğlu, A. Kara and T.S. Rahman, Phy. Rev. B.67, 235405 (2003).
- [46].T.S. Chen, G.P. Alldredge and F.W. De Wette, Surf. Sci. 62, 675 (1977).
- [47].H. Yildirim, A. Kara, S. Durukanoğlu and T. S Rahman, Surf. Sci.600, 484 (2006).
- [48].J. Hertz, J. Phys. IV France.122, 3 (2004)
- [49].L. Dobrzynski and J. Friedel, Surf. Sci.12, 469 (1968).
- [50].F. X. Timmes and F. D. Swesty, The Astrophy. J. Supplement Series.126, 501 (2000).
- [51].A. Kara and T. S. Rahman, Surf. Sci. Reports. 56, 159 (2005).
- [52].S. Durukanoğlu, A. Kara and T.S. Rahman, Phy. Rev. B.55, 13894 (1997).
- [53].A. A. Maradudin and R. F. Wallis, Phy. Rev. 148, 945 (1966).
- [54]. V.A. Khodel, J.W. Clark, V.R. Shaginyan and M.V. Zverev, JETP Letters. 92, 532 (2010).
- [55].M. L. Klein, G. K. Horton and J. L. Feldman, Phy. Rev. 184, 968 (1969).
- [56].A. Van de Walle and G. Ceder, Rev. Mod. Phys. 74, 11 (2002).
- [57].A. Einstein, Annalen der Physik.22, 180 (1907).
- [58].P. Debye, Annalen der Physik. 39, 789 (1912).
- [59].J.P. Poirier, Introduction to the physics of the earth's interior, Edition 2, Cambridge University Press, (2000).
- [60]P. Brüesch, Phonons: Theory and Experiments I, Lattice Dynamics and Models of Interatomic Forces, Springer-Verlag Berlin Heidelberg New York (1982).
- [61] P. F. Lory, Dynamique de réseau et conductivité thermique dans les alliages métalliques complexes, thèse doctorat. Université Grenoble Alpes (2015).